Interaction between the chain and ladder subsystems in $(Ca,Sr,La)_{14}Cu_{24}O_{41}$ compounds

2008 J. Phys.: Condens. Matter 20 382201

(http://iopscience.iop.org/0953-8984/20/38/382201)

IOP FTC
IOP PUBLISHING JOURNAL OF PHYSICS: CONDENSED MATTER
J. Phys.: Condens. Matter **20** (2008) 382201 (5pp) doi:10.1088/0953-8984/20/38/382201

FAST TRACK COMMUNICATION

Interaction between the chain and ladder subsystems in (Ca, Sr, La)$_{14}$Cu$_{24}$O$_{41}$ compounds

U Schwingenschlögl[1,2] **and C Schuster**[1]

[1] Institut für Physik, Universität Augsburg, D-86135 Augsburg, Germany
[2] ICCMP, Universidade de Brasília, 70904-970 Brasília, DF, Brazil

Received 10 July 2008
Published 21 August 2008
Online at stacks.iop.org/JPhysCM/20/382201

Abstract
We investigate the influence of structural modulations on the electronic properties of incommensurate (Ca, Sr, La)$_{14}$Cu$_{24}$O$_{41}$ compounds by band structure calculations based on density functional theory and the local density approximation (LDA). Using a supercell approach with ten CuO_2 chain and seven Cu_2O_3 ladder segments, we take into account the major effects of the structural incommensurability. We find that the LDA electronic states show very little response to these modulations. The coupling between the electronic and structural degrees of freedom, hence, can be well described in terms of two independent subsystems. The incommensurate charge density waves (CDWs) in the chains and the ladders are formed independently of each other.

(Some figures in this article are in colour only in the electronic version)

The isostructural spin-chain compounds $M_{14}Cu_{24}O_{41}$ (M = Ca, Sr, La) have been the subject of intensive research in recent years, mainly due to their rich phase diagram and close relations to the high-T_c cuprates. Their incommensurate crystal structures consist of planes of quasi-one-dimensional CuO_2 chains stacked alternately with planes of two-leg Cu_2O_3 ladders. The orientation of the chains (or ladders) defines the crystallographic c-axis, where the lattice constants of these two subsystems satisfy in a good approximation $10c_{\text{chain}} \approx 7c_{\text{ladder}}$ [1]. The copper ions are intrinsically hole doped with nominal Cu valence +2.25 for both the Ca and the Sr compound. However, the ladders accommodate fewer holes than the chains, leading to a Cu valence of about +2.50, which is related to a sequence of Cu^{3+} ($S = 0$) and Cu^{2+} ($S = 1/2$) ions in the chains and corresponds to a quarter filled Hubbard band [2, 3]. Optical conductivity and x-ray absorption experiments suggest that the substitution of Ca for Sr induces a transfer of holes from the chains to the ladders [4]. On La substitution the intrinsic doping is reduced, reaching the undoped state with nominal Cu valence +2.00 in the $La_6Ca_8Cu_{24}O_{41}$ case. A big spin gap makes the Cu_2O_3 ladders magnetically inert, whereas the magnetic phase diagram of the CuO_2 chains is quite rich and attracts a lot of attention. Despite this strong doping dependence [5–8], the materials stay isostructural [9–11]. While the CuO_2 chains are non-magnetic with a spin gap of about 130 K for $Sr_{14}Cu_{24}O_{41}$ [12], antiferromagnetic ordering is reported for Ca rich samples [13, 14]. Ferromagnetism, as expected for a Cu–O–Cu bond angle of approximately 90°, is realized in La rich systems. The origin of the intrachain antiferromagnetic order in the case of a quarter filled band, however, is a more difficult question due to a complicated interplay of ordering effects [15].

First principles band structure calculations for a simplified unit cell of $Sr_{14}Cu_{24}O_{41}$ have been performed by Arai *et al* [16]. Moreover, the influence of the characteristic modulations in the structure of the CuO_2 chains in $Sr_{14-x}Ca_xCu_{24}O_{41}$ on the on-site and nearest neighbour effective parameters has been determined by Gellé and Lepetit [17], likewise applying an *ab initio* approach. The modulations appear to be of central importance for effects like the electron localization and the magnetic ordering in the CuO_2 chains, since the on-site orbital energies and intrachain hopping parameters strongly vary as function of the incommensurability parameter. A second neighbour t–J + V model has been extracted from *ab initio* results in [18]. X-ray diffraction

data indicate that holes localize at low temperature in the potential given by the structural modulation, which, in turn, leads to a further deformation of the lattice [19]. Inelastic light scattering experiments by Choi *et al* [20] point towards a complicated interplay between the lattice distortions and electronic correlations, affecting the incommensurate CDWs within the CuO_2 chains and Cu_2O_3 ladders. The origin of these CDWs, however, is an open problem, since they either can be traced back to the incommensurate interaction between chains and ladders or may be intrinsic to these subsystems. The present paper aims at solving this question. Due to a recent structure refinement, we will study in detail $Sr_{14}Cu_{24}O_{41}$. Our results do not depend on this choice but can be transferred to related systems, which is checked for both $Ca_{14}Cu_{24}O_{41}$ and $La_6Ca_8Cu_{24}O_{41}$. We show that the band structure of the CuO_2 chains is well described in terms of a tight-binding model, for which we deduce explicit parameters. As a consequence, the electronic states are not affected by the modulations of the chain–ladder interaction, but incommensurate CDWs are formed independently on the chains and ladders.

Our electronic structure calculations for $Sr_{14}Cu_{24}O_{41}$ rely on the scalar-relativistic augmented spherical wave (ASW) method [21]. This method has proven to be suitable for dealing with unit cells comprising a large number of atomic sites [22–24]. We use a recently improved implementation of the ASW code, which accounts for the non-spherical contributions to the charge density inside the atomic spheres [25]. In particular, our calculations take into account the structural incommensurate modulations characteristic of spin-chain compounds via a periodic approximation of the unit cell, comprising ten chain and seven ladder units. Structural parameters are taken from [1]. For identifying the specific effects of the chain–ladder interaction, both the chains and ladders are modelled as a sequence of (ten and seven, respectively) identical building blocks. That is, we suppress the modulations within each of the two subsystems, in order to judge whether they are intrinsic features or can be traced back to the chain–ladder interaction. Because a unit cell contains two formula units, we have to deal with 28 M, 48 Cu, and 82 O atomic spheres. To optimize the basis sets, 130 additional augmentation spheres are placed at carefully selected interstitial sites. In the following, we will focus on the prototypical compound $Sr_{14}Cu_{24}O_{41}$, which is discussed in the literature most frequently. Our findings for the Ca and La system are closely related and fully support our conclusions. In the present case the basis set for the secular matrix comprises Sr 5s, 5p, 4d, Cu 3d, 4s, 4p, and O 2s, 2p orbitals, as well as states of the additional augmentation spheres. Moreover, the Brillouin zone integrations are performed using a growing number of up to 24 **k**-points in the irreducible wedge. The Vosko–Wilk–Nusair parametrization is applied for the exchange–correlation functional.

In figure 1 we address the partial Cu 3d density of states (DOS) of the CuO_2 chains in $Sr_{14}Cu_{24}O_{41}$, normalized with respect to the number of contributing sites. A finite DOS at the Fermi energy contradicts the experimental observation of a non-metallic state. In order to reproduce the insulating behaviour, it would be necessary to treat the

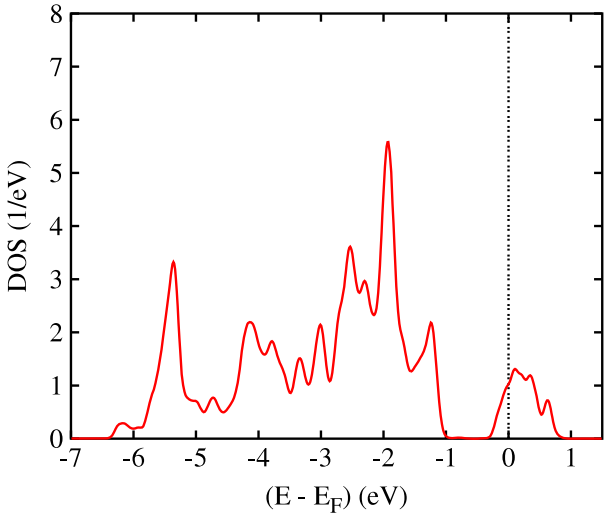

Figure 1. Partial Cu 3d density of states (per Cu atom) for the chain subsystem of $Sr_{14}Cu_{24}O_{41}$.

electron–electron interaction more adequately, hence to go beyond the local density approximation. However, for our present purpose (of quantifying the chain–ladder interaction) electronic correlations do not play a critical role. States in the energy range considered in figure 1 are composed of Cu 3d and O 2p orbitals, indicating strong intrachain Cu–O hybridization. The Cu 3d DOS reveals a distinct structure with a width of about 1 eV around the Fermi level, separated by a gap of likewise 1 eV from the remaining valence bands. States close to the Fermi level have almost pure Cu $3d_{xz}$ symmetry. As to be expected, they mediate the main part of the intrachain Cu–O orbital overlap and are associated with bands near quarter filling. Therefore, they are subject to a large variety of possible ordering processes of the charge and spin degrees of freedom [3]. Contributions of other states amount to less than 0.1% of the total DOS at the Fermi energy. For establishing further insight into the electronic structure of the CuO_2 chains, we turn to the band structure data underlying the DOS curve of figure 1. Weighted electronic bands as calculated for $Sr_{14}Cu_{24}O_{41}$ are shown in figure 2 in the periodic zone scheme. The bands are given along the high symmetry line Γ–Z, which (in real space) corresponds to the direction of the CuO_2 chains. Starting at the Γ-point, the **k**-range covers five Brillouin zones. In addition, the width of the bars given for every band and **k**-point represents the admixtures of the Cu $3d_{xz}$ states. Bands with minor Cu $3d_{xz}$ contributions are not shown for clarity. By means of a periodic zone scheme, we can address the periodicity of the electronic states. We have $\mathbf{k}_\Gamma = (0, 0, 0)$ as well as $\mathbf{k}_Z = (0, 0, 2\pi/c_{\text{chain}})$, where the length of one chain segment amounts to $c_{\text{chain}} = 2.75$ Å. Surprisingly, a reasonable fit of the band structure data needs nothing but a tight-binding dispersion

$$\epsilon(k_z) = \epsilon_0 - 2t_1 \cos(k_z c_{\text{chain}}) - 2t_2 \cos(2k_z c_{\text{chain}}) - 2t_3 \cos(3k_z c_{\text{chain}}), \quad (1)$$

where k_z is the z-component of the reciprocal lattice vector and ϵ_0 is the band centre. The nearest, next-nearest, and next-next-nearest neighbour intrachain hopping parameters are

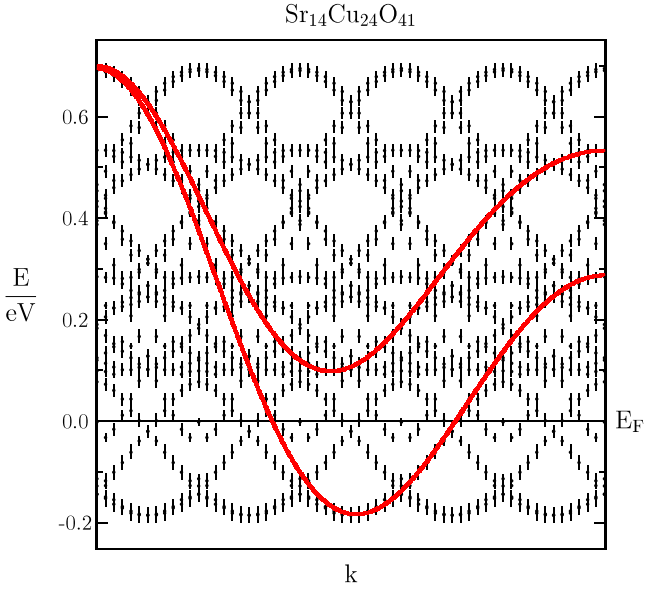

Figure 2. Electronic bands of $Sr_{14}Cu_{24}O_{41}$ in the periodic zone scheme. The bands are shown along the high symmetry line Γ–Z, which is the direction of the CuO_2 chains in real space. Starting at the Γ-point, the **k**-range covers five Brillouin zones, where bands with minor Cu $3d_{xz}$ admixture are not depicted.

Table 1. Tight-binding parameters for the Cu $3d_{xz}$ bands of $Sr_{14}Cu_{24}O_{41}$, $Ca_{14}Cu_{24}O_{41}$, $La_6Ca_8Cu_{24}O_{41}$, and both CuO_2 model chains.

	Sr_{14}	Ca_{14}	La_6Ca_8	Unsymm.	Symm.
			Band 1		
t_1 (eV)	0.163	0.16	0.15	0.240	0.185
t_2 (eV)	0.336	0.40	0.37	0.335	0.360
t_3 (eV)	0.040	0.03	0.03	0.035	0.025
$t_\perp$ (eV)					0.030
ϵ_0 (eV)	0.155	0.15	0.01	1.45	1.45
			Band 2		
t_1 (eV)	0.028	0.03	0.03	0.115	0.090
t_2 (eV)	0.254	0.25	0.26	0.235	0.230
t_3 (eV)	0.055	0.03	0.02	0.045	0.060
$t_\perp$ (eV)					0.140
ϵ_0 (eV)	0.362	0.43	0.25	1.67	1.56

denoted as t_1, t_2, and t_3, respectively. The bands resulting from the tight-binding fit are illustrated in figure 2 via broad lines, and corresponding fit parameters are summarized in table 1. Competence between nearest and next-nearest neighbour interactions is a well known phenomenon in this material class [26, 27].

The spin-chain systems $M_{14}Cu_{24}O_{41}$ can be described in terms of three largely independent subsystems: CuO_2 chains, Cu_2O_3 ladders, and the electron donor system of M ions which separates chains and ladders. Hybridization between atomic orbitals belonging to different subsystems is negligible as the valence states of the M ions are almost fully depopulated. The electronic structure of coupled CuO_2 chains without incommensurate modulation consequently can be addressed by means of a model system consisting of two CuO_2

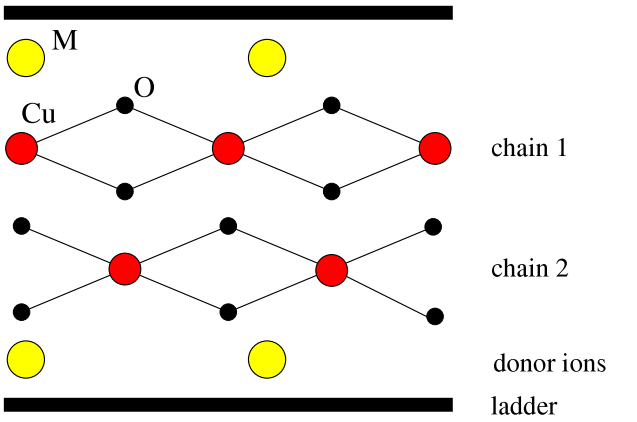

Figure 3. Schematic arrangement of the coupled CuO_2 chains in the symmetrical configuration.

units [15]. Importantly, neither the structural modulations nor the relaxation of the oxygen positions in the original system are found to enhance the chain–ladder coupling. Different spin-chain compounds are distinguished by a relative shift between adjacent chains with respect to the chain axis. While for $Ca_{13.6}Sr_{0.4}Cu_{24}O_{41}$ the chains are shifted by half the intrachain Cu–Cu distance for example, a shift of only 30% of the Cu–Cu distance remains for $Sr_{14}Cu_{24}O_{41}$. For convenience, we call these two cases the symmetrical (see the schematic representation in figure 3) and unsymmetrical configuration of the coupled chains, respectively.

The upper panel of figure 4 shows partial Cu 3d densities of states for these two model systems, where the curves resemble the essential features of the $Sr_{14}Cu_{24}O_{41}$ DOS; see figure 1. Close to the Fermi energy even all the details of the DOS curves fully coincide. We have a widespread structure with a width of 5.2 eV at lower energies and a structure extending over a range of some 1 eV at higher energies. However, the model DOS is subject to a rigid band shift of 1.3 eV to higher energies, as the M ions are not taken into account. The characteristic antibonding combination of Cu $3d_{xz}$ and O $2p_x/2p_z$ orbitals therefore is found in the energy range from 1.1 to 2.1 eV. Further insights into the properties of the model system result from the band structure data in the lower panel of figure 4 for the unsymmetrical arrangement of the coupled CuO_2 chains (as relevant for $Sr_{14}Cu_{24}O_{41}$). Comparison with figure 2 reveals an excellent accordance with the band structure of the real system. The tight-binding parameters summarized in table 1 support this conclusion.

Our results nicely confirm a strongly suppressed nearest neighbour hopping, since t_1 is found to be very small. This property of spin-chain compounds can be traced back to a Cu–O–Cu bond angle close to 90° [26, 27]. Moreover, we note that a relative shift between adjacent chains affects the interchain hopping $-t_\perp \cos(0.5 k_z c_{\text{chain}})$. Whereas we find for unsymmetrical chains a reasonable fit for $t_\perp = 0$, a finite $t_\perp$ is necessary for symmetrical chains. In fact, enhanced interchain coupling is expected in the latter case due to an increased orbital overlap.

As a consequence of the even quantitative agreement of the electronic states in our model CuO_2 chain and in the

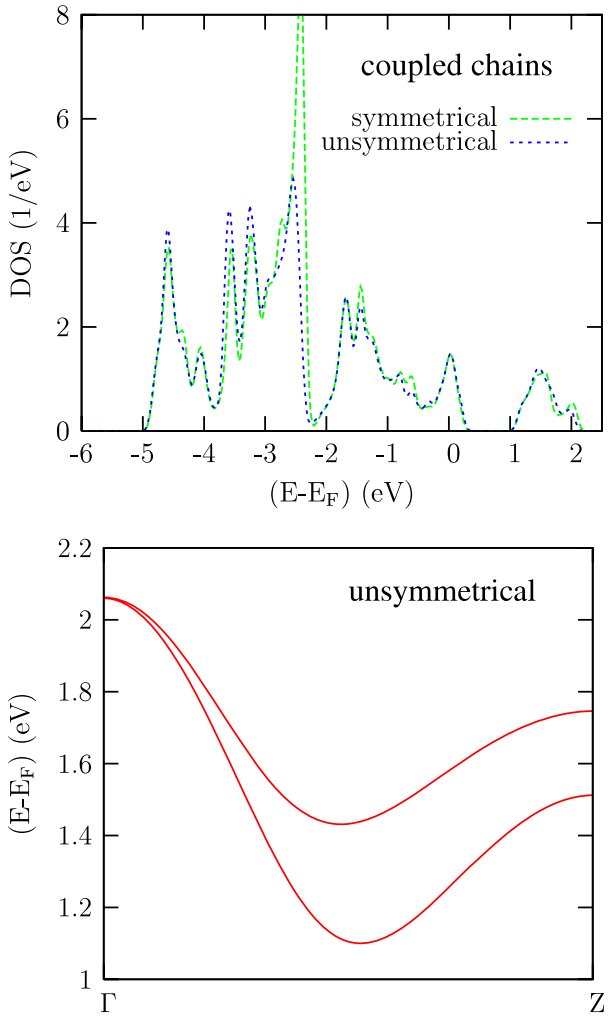

Figure 4. Partial Cu 3d densities of states (per copper atom) for CuO_2 model chains coupled symmetrically and unsymmetrically. The band structure refers to the Cu 3d bands of the unsymmetrical case, as realized in $Sr_{14}Cu_{24}O_{41}$. The electronic states of the model systems are subject to rigid band shifts of 1.3 eV, as compared to the real system.

CuO_2 subsystem of the real $Sr_{14}Cu_{24}O_{41}$ structure, one can judge the influence of the chain–ladder interaction in spin-chain compounds: the interaction between the subsystems is much too weak to cause the observed incommensurability of the electronic structure. A modulation of orbital parameters thus cannot result from the structural incommensurability of the two basic building units, but has to be an intrinsic property of the ingredients. Due to charge transfer off the electron donor ions as well as between chains and ladders, a state of incommensurate doping is created. Any instability against incommensurate CDWs, however, must be inherent to the CuO_2 chains and Cu_2O_3 ladders, independent from each other. Spin-chain compounds thus are well described in terms of two independent incommensurate CDWs. Note that other cuprate systems with essentially independent chains cannot be expected to exhibit the same instability due to differences in the bonding details.

In summary, we have studied the electronic properties of the spin-chain system $M_{14}Cu_{24}O_{41}$ (M = Ca, Sr, La) by means of density functional theory. Taking into consideration the structural incommensurabilities of the CuO_2 chain and Cu_2O_3 ladder subsystems in the prototypical compound $Sr_{14}Cu_{24}O_{41}$, we have established insight into the electronic structure. Because hybridization between the chains, the ladders, and the electron donor M ions is negligible, the band structure of the CuO_2 chains could be compared to a model system without chain–ladder interaction. It turns out that the real and model systems agree excellently as concerns their band structure. As a consequence, one can conclude that the electronic states of the CuO_2 chains, like those of the Cu_2O_3 ladders, do not respond to the structural modulation induced by the respective other subsystem. The observed strong modulations of the on-site and hopping parameters thus are identified as intrinsic features of the chains and ladders, traced back to an incommensurate band filling. Finally, because the spin-chain compounds are closely related to each other with respect to the chain–ladder coupling, we expect that our results for $(Ca, Sr, La)_{14}Cu_{24}O_{41}$ apply to the whole class of materials, clarifying the origin of the observed incommensurability.

We thank U Eckern and P Schwab for several helpful discussions and the Deutsche Forschungsgemeinschaft for financial support (SFB 484).

References

[1] Gotoh Y, Yamaguchi I, Takahashi Y, Akimoto J, Goto M, Onoda M, Fujino H, Nagata T and Akimitsu J 2003 *Phys. Rev.* B **68** 224108
[2] Nücker N, Merz M, Kuntscher C A, Gerhold S, Schuppler S, Neudert R, Golden M.S, Fink J, Schild D, Stadler S, Chakarian V, Freeland J, Idzerda Y U, Conder K, Uehara M, Nagata T, Goto J, Akimitsu J, Motoyama N, Eisaki H, Uchida S, Ammerahl U and Revcolevschi A 2000 *Phys. Rev.* B **62** 14384
[3] Schuster C and Schwingenschlögl U 2007 *Phys. Rev.* B **75** 045124
[4] Osafune T, Motoyama N, Eisaki H and Uchida S 1997 *Phys. Rev. Lett.* **78** 1980
[5] Carter S A, Batlogg B, Cava R J, Krajewski J J, Peck W F Jr and Rice T M 1996 *Phys. Rev. Lett.* **77** 1378
[6] Ammerahl U, Büchner B, Colonescu L, Gross R and Revcolevschi A 2000 *Phys. Rev.* B **62** 8630
[7] Braden M, Etrillard J, Gukasov A, Ammerahl U and Revcolevschi A 2004 *Phys. Rev.* B **69** 214426
[8] Kataev V, Choi K-Y, Grüninger M, Ammerahl U, Büchner B, Freimuth A and Revcolevschi A 2001 *Phys. Rev.* B **64** 104422
[9] Ohta T, Izumi F, Onoda M, Isob M, Takayama-Muromachi E and Hewat A W 1997 *J. Phys. Soc. Japan* **66** 3107
[10] Matsuda M, Katsumata K, Osafune T, Motoyama N, Eisaki H, Uchida S, Yokoo T, Shapiro S M, Shirane G and Zarestky J L 1997 *Phys. Rev.* B **56** 14499
[11] Klingeler R 2003 Spin- und Ladungsordnung in Übergangsmetalloxiden—Thermodynamische und magnetische Untersuchungen *Dissertation* (RWTH Aachen)
[12] Matsuda M and Katsumata K 1996 *Phys. Rev.* B **53** 12201
[13] Nagata T, Fujino H, Akimitsu J, Nishi M, Kakurai K, Katano S, Hiroi M, Sera M and Kobayashi N 1999 *J. Phys. Soc. Japan* **68** 2206
[14] Isobe M, Onoda M, Ohta T, Izumi F, Kimoto K, Takayama-Muromachi E, Hewat A W and Ohoyama K 2000 *Phys. Rev.* B **62** 11667
[15] Schwingenschlögl U and Schuster C 2007 *Europhys. Lett.* **79** 27003

Schwingenschlögl U and Schuster C 2007 *Phys. Rev. Lett.* **99** 237206
[16] Arai M and Tsunetsugu H 1997 *Phys. Rev.* B **56** R4305
[17] Gellé A and Lepetit M-B 2004 *Phys. Rev. Lett.* **92** 236402
[18] Gellé A and Lepetit M-B 2005 *Eur. Phys. J.* B **46** 489
[19] Zimmermann M v, Geck J, Kiele S, Klingeler R and Büchner B 2006 *Phys. Rev.* B **73** 115121
[20] Choi K-Y, Grove M, Lemmens P, Fischer M, Güntherodt G, Ammerahl U, Büchner B, Dhalenne G, Revcolevschi A and Akimitsu J 2006 *Phys. Rev.* B **73** 104428
[21] Eyert V 2000 *Int. J. Quantum Chem.* **77** 1007
[22] Schwingenschlögl U, Eyert V and Eckern U 2003 *Europhys. Lett.* **61** 361
[23] Schmitt T, Augustsson A, Nordgren J, Duda L-C, Höwing J, Gustafsson T, Schwingenschlögl U and Eyert V 2005 *Appl. Phys. Lett.* **86** 064101
[24] Schwingenschlögl U and Schuster C 2006 *Chem. Phys. Lett.* **432** 245
[25] Eyert V 2007 *The Augmented Spherical Wave Method—A Comprehensive Treatment* (*Springer Lecture Notes in Physics*) (Heidelberg: Springer)
[26] Tornow S, Entin-Wohlman O and Aharony A 1999 *Phys. Rev.* B **60** 10206
[27] Drechsler S-L, Volkova O, Vasiliev A N, Tristan N, Richter J, Schmitt M, Rosner H, Malek J, Klingeler R, Zvyagin A A and Büchner B 2007 *Phys. Rev. Lett.* **98** 77202